Redox Biology 58 (2022) 102524

Contents lists available at ScienceDirect

Redox Biology

journal homepage: www.elsevier.com/locate/redox

Nanoparticle endothelial delivery of PGC-1α attenuates hypoxia-induced pulmonary hypertension by attenuating EndoMT-caused vascular wall remodeling

Dunpeng Cai [a], Shi-You Chen [a,b,*]

[a] Departments of Surgery, University of Missouri School of Medicine, Columbia, MO, USA
[b] Department of Medical Pharmacology & Physiology, University of Missouri School of Medicine, Columbia, MO, USA

ARTICLE INFO

Keywords:
Pulmonary hypertension
Peroxisome proliferator-activated receptor gamma coactivator-1α
Endothelial to mesenchymal transition
Nitric oxide

ABSTRACT

Pulmonary hypertension (PH) induced by chronic hypoxia is characterized by thickening of pulmonary artery walls, elevated pulmonary vascular resistance, and right-heart failure. Dysfunction of endothelial cells is the hallmark event in the progression of PH. Among various mechanisms, endothelial to mesenchymal transition (EndoMT) has emerged as an important source of endothelial cell dysfunction in PH. However, the mechanisms underlying the EndoMT in PH remain largely unknown. Our results showed that peroxisome proliferator-activated receptor gamma coactivator 1-alpha (PGC-1α) expression was decreased in pulmonary arterial endothelial cells (PAECs) in PH patients and hypoxia-induced PH mouse model compared to the normal controls. Endothelial-specific overexpression of PGC-1α using nanoparticle delivery significantly attenuated the progression of PH, as shown by the significantly decreased right ventricular systolic pressure and diminished artery thickness as well as reduced vascular muscularization. Moreover, Endothelial-specific overexpression of PGC-1α blocked the EndoMT of PAECs during PH, indicating that loss of PGC-1α promotes PH development by mediating EndoMT, which damages the integrity of endothelium. Intriguingly, we found that PGC-1α overexpression rescued the expression of endothelial nitric oxide synthase in mouse lung tissues that was deceased by hypoxia treatment *in vivo* and in endothelial cells treated with TGF-β *in vitro*. Consistently, PAECs and vascular smooth muscle co-culture showed that overexpression of PGC-1α in PAECs increases nitric oxide release, which would likely diffuse to smooth muscle cells, where it activates specific protein kinases, and initiates SMC relaxation by diminishing the calcium flux. Endothelial-specific overexpression of PGC-1α also attenuated hypoxia-induced pulmonary artery stiffness which appeared to be caused by both the decreased endothelial nitric oxide production and increased vascular remodeling. Taken together, these results demonstrated that endothelial-specific delivery of PGC-1α prevents PH development by inhibiting EndoMT of PAECs and thus restoring endothelial function and reducing vascular remodeling.

1. Introduction

Pulmonary arterial hypertension (PAH) is a progressive condition. The 1-, 2-, and 3-year mortality rates in the United States are 8%, 16%, and 21%, respectively [1].The pathogenesis of PAH is characterized by progressive increases in pulmonary vascular resistance and pulmonary artery pressure (>25 mmHg at rest) due to pulmonary vascular remodeling, endothelial dysfunction, impaired vasoconstriction, and intravascular thrombosis [2–4]. Currently, treatment options are limited, and lack of treatment can lead to right heart failure and premature lethality. Current pharmacological therapies targeting abnormalities in the prostacyclin, nitric oxide, and endothelin pathways can improve PAH symptoms and lead to modest survival benefits, but do not reverse the disease pathogenesis. Until now, lung transplantation remains the best option for this devastating disease. Thus, it's becoming clinically urgent to identify novel therapeutic targets for PAH.

Pathological studies indicate that aberrant vascular remodeling implicated in the increased pulmonary vascular resistance include concentric arterial wall thickening, occlusive intimal lesions, and neo muscularization of precapillary arterioles [5]. Concentric pulmonary vascular wall thickening is characterized by significant intimal and medial hypertrophy due to dysfunction of pulmonary artery endothelial cells (PAECs) and elevated proliferation/attenuated apoptosis of SMCs

* Corresponding author. Department of Surgery University of Missouri School of Medicine, 1 Hospital Drive, Columbia, MO, 65212, USA.
E-mail address: scqvd@missouri.edu (S.-Y. Chen).

https://doi.org/10.1016/j.redox.2022.102524
Received 30 September 2022; Received in revised form 21 October 2022; Accepted 24 October 2022
Available online 28 October 2022

Abbreviations

PH	Pulmonary hypertension
PAH	Pulmonary artery hypertension
EndoMT	Endothelial to mesenchymal transition
PGC-1α	peroxisome proliferator-activated receptor gamma coactivator 1-alpha
NO	nitric oxide
eNOS	Nitric oxide synthase
PAECs	Pulmonary arterial endothelial cells
SMC	Smooth muscle cells
VE-cadherin	Vascular endothelial cadherin
TGF-β	Transforming growth factor β
TEER	Trans endothelial Electrical Resistance
PWV	Pulse wave velocity
RV/LV + S	Ventricular to Left Ventricular Diameter Ratio at End-Systole
α-SMA	α-smooth muscle actin
FITC	Fluorescein isothiocyanate

[6]. Although the mechanism underlying PAH is not fully understood, endothelial dysfunction, loss of endothelial cell integrity, infiltration of immune cells is identified as the major players in the development and progression of vascular pathology in PAH [7]. Numerous studies have shown that endothelial dysfunction and loss of endothelial cell integrity are associated with endothelial-mesenchymal transition (EndoMT). EndoMT is a process by which ECs acquire a mesenchymal phenotype in association with the downregulation of EC-specific genes, such as platelet EC adhesion molecule 1 (CD31) and vascular endothelial cadherin (VE-cadherin), and with the upregulation of mesenchymal-specific genes, such as α-SMA and fibroblast-specific genes like vimentin [8]. During the EndoMT, ECs lose their junctions to the endothelium and gain migratory and proliferative capacities as they gradually switch from endothelial to a mesenchymal phenotype [9]. The molecular mechanisms inducing EndoMT in PAH remain elusive with several signaling pathways implicated. For example, the transforming growth factor β (TGF-β) signaling pathway is critical for PAH development and is also an important player in EndoMT [10–12]. TGF-β induces α-SMA and type I collagen expression while downregulating VE-cadherin expression in PAECs. EndoMT may cause endothelial cell dysfunction and increase vascular permeability which could lead to enhanced immune cell infiltration. Importantly, EndoMT may be a reversible biological process, what is called mesenchymal-to-endothelial transition, suggesting that exploration of the regulatory mechanism of the reversible process of EndoMT will provide new insights into the prevention and treatment of PAH.

In healthy individuals, the prevention of pulmonary vascular remodeling and the preservation of a normal pulmonary tension appear to be controlled by Nitric oxide (NO) signaling. NO production by ECs is a key defense mechanism against vascular dysfunction across multiple vascular beds, including the pulmonary circulation [13]. In ECs, NO production occurs primarily via endothelial nitric oxide synthase (eNOS). The endothelial derived NO diffuse from EC to SMCs, where it activates specific protein kinases, and initiate SMC relaxation [14]. However, endothelial dysfunction causes decrease in NO bioavailability and variations in the release of vasoactive compounds [15]. In the development of PAH, the deceased eNOS expression in endothelium is identified in both human patients and experimental pulmonary hypertension mouse model [16,17], and the NO synthesis and multiple signaling pathways are disrupted or altered in pulmonary vascular diseases. Although further studies are needed to determine to what extent these derangements contribute to the pathogenesis of PAH, modification of the deficiency in NO synthesis has been shown to attenuate pulmonary vascular remodeling, and this strategy appears to be effective in the treatment of PAH and neonatal pulmonary hypertension [18]. However, additional studies are needed to identify methods to effectively enhance NO synthesis in endothelial cells.

Peroxisome proliferator activated receptor gamma coactivator 1α (PGC-1α) is a unique stress sensor that largely acts to promote adaptive responses in endothelial cells. PGC-1α is involved in the regulation of antioxidant defense, anti-apoptosis, anti-inflammatory properties, and mitochondrial biogenesis in endothelial cells. Furthermore, overexpressing PGC-1α improves endothelium-dependent relaxation and preserves eNOS coupling [19]. Although studies have shown that suppression of PGC-1α is associated with hypoxia-induced endothelial dysfunction in PAH [20,21], PGC-1α function in pulmonary hypertension (PH) remains to be determined experimentally. Endothelial PGC-1α is reported to mediate EndoMT in diabetes [22], and there are reports showing that PGC-1α dictates endothelial function through regulation of eNOS expression [23,24]. However, it remains unknown if PGC-1α can ameliorate EndoMT of PAECs. To clearly determine the function of PGC-1α in PH and EndoMT, we overexpressed PGC-1α using a nanoparticle delivery of endothelial-specific promoter driven plasmid to PAECs. Our results showed that overexpression of PGC-1α ameliorates PH by blocking EndoMT and reducing pulmonary artery stiffness via enhancing the expression of eNOS in PAECs.

2. Materials and methods

2.1. Cell culture

Human PAECs were purchased from Lifeline Cell Technology (FC-0055) and cultured using vascular endothelial growth factor-contained endothelial medium (LL-0003) under 37 °C, 5% CO_2 conditions. The cells at passages 3–5 were used in this study. The cultured PAECs were treated with TGF-β (5 ng/ml, R&D Systems 7754-BH) to induce EndoMT.

2.2. Chronic hypoxia-induced pulmonary hypertension model in mice

Eight-to 10-week-old C57BL6 male mice were administrated (i.v) with nanoparticles (MountView Therapeutics) containing control vector or PGC-1 *α* expression plasmid were exposed to room air (normoxia) or 10% oxygen (hypoxia) in a ventilated chamber, as described previously [25]. All animals had free access to standard chow diet and water and were subjected to an alternating 12-h light/12-h dark cycle under controlled environment. The chamber was opened twice a week for 10–15 min for cleaning and supplementing food and water. After 4 weeks, pulmonary hypertension and pulmonary vascular remodeling were assessed.

2.3. Western blot analysis

Lung tissues or PAECs were lysed in RIPA buffer (50 mM Tris-HCl, pH 7.4, 1% Triton X-100, 0.25% w/v sodium deoxycholate, 150 mM NaCl, 1 mM EGTA, 0.1% SDS, protease inhibitor cocktail). The lysates were centrifugated, and supernatants were collected. Protein concentrations were measured using BCA Protein Assay Reagent (Thermo Scientific). Equal amounts of proteins (5–20 μg) were resolved in 9% or 14% SDS-PAGE and were transferred to polyvinylidene difluoride membranes (Bio-Rad). Antibodies against PGC-1α (1:1000, 2178, Cell signaling), N-cadherin (1:1000, Zymed 18–0224), vimentin (1:1000, Invitrogen MA3-745), VE-cadherin (1:500, Santa Cruz Biotechnology sc-28644), CD31 (1:500, Santa Cruz Biotechnology sc-376764), α-SMA (1:3000, 19245S, Cell signaling) and GAPDH (1:10000, Proteintech) were used for immunoblotting. Corresponding secondary antibodies (anti-mouse IgG, 926–68072 (680RD) or 926–32212 (800CW); or anti-rabbit IgG, 926–68073 (680RD) or 926–32213 (800CW); 1:10,000 dilution, Li-Cor Biosciences) were incubated for 1 h at room temperature. Protein bands

were detected and analyzed on an Odyssey CLx Imager with Image Studio software (v.4.0; Li-Cor Biosciences).

2.4. Histochemistry and immunohistology analysis

After fixing in 4% paraformaldehyde overnight, the mouse lungs were dehydrated in a graded series of ethanol and xylene solutions, embedded in paraffin, and sectioned (5 μm). The sections were deparaffinized in xylene and rehydrated. Hematoxylin and eosin (H&E) staining was performed with an H&E Stain Kit (KTHNEPT; American Mastertech Scientific) according to the manufacturer's instructions. For immunohistochemical staining, the sections undergoing microwave antigen retrieval in 10 mM citrate buffer (pH 6.0) were allowed to cool down to room temperature followed by washing with PBS. The endogenous peroxidase activity was quenched by the addition of 3% H_2O_2. Subsequently, slides were washed with PBS, and nonspecific antibody binding was blocked by incubation with 10% goat serum for 30 min. The sections were then incubated with PGC-1α primary antibody (1:100) or corresponding normal IgG (negative control) at 4 °C overnight followed by incubation with horseradish peroxidase-conjugated secondary antibody (1:200). The sections were counterstained with hematoxylin. Images were captured with a CCD camera mounted on a microscope (Nikon, Tokyo, Japan). Quantification was performed with the ImageJ Immunohistochemistry Image Analysis Toolbox (NIH). Pulmonary distal arteriole (outside diameter between 20 and 70 μm) muscularization was defined as described previously [26]: non-muscular (no evidence of vessel wall muscularization) or muscular (i.e., partially muscular (SMCs identifiable in less than three-fourths of the vessel circumference) or fully muscular (SMCs in more than three-fourths of the vessel circumference)). For each animal, at least 10 fields for each section were examined at a 100-fold magnification. To evaluate the medial wall thickness, Van Gieson's staining was performed using Elastic stain kit (Sigma, HT25A-1 KT). The relative wall thickness was defined as (external diameter-internal diameter)/external diameter x100. About 10 pulmonary arteries (outside diameter between 20 and 70 μm) were examined at a 200-fold magnification in each lung section.

For immunofluorescent staining, the hydrated sections underwent microwave antigen retrieval as described above, washed with PBS, and blocked with 10% goat serum for 30 min at room temperature, followed by incubation with PGC-1α (1:100), Vwf (1:100, 11778-1-AP, Proteintech), Vimentin (ab92547, Abcam) CD31 (1:100, sc-376764; Santa Cruz Biotechnology) primary antibody at 4 °C overnight. Then, the sections were incubated with FITC (fluorescein isothiocyanate)- or TRITC (tetramethylrhodamine-isothiocyanate)- labeled secondary antibody (1:100) at room temperature for 1 h. Nuclei were stained with DAPI (4′,6-diamidino-2-phenylindole, H-1500; Vector Laboratories). Fluorescent images were captured using a Confocal microscopy (Nikon Ti Eclipse with A1R scan head).

2.5. Plasmids construction and transfection

Full-length human PGC-1α cDNA was obtained by PCR amplification from human total RNA reverse transcription using primers containing restriction enzyme sites for XhoI (R0146S, NEB) and NdeI (R0111S, NEB). The primers used were CTC GAG AGT AAG GGG CTG GTT GCC (forward) and CAT ATG TAG ATT TGA AAC A TT CTT TTC CCT (reverse). The cDNA fragments were digested with restriction enzymes and cloned into the pGL3CDH5p-eGFP vector. The PGC-1α cDNA insertion in the plasmid was confirmed by DNA sequencing. The plasmid was transiently transfected into PAECs using jetPRIME transfection reagent (Polyplus transfection) according to the manufacturer's instruction. For administration into mice *in vivo*, nanoparticles containing plasmids were prepared as described previously [27]. Briefly, empty plasmids or PGC-1α expression plasmids were mixed with PP/PEI nanoparticles (#EndoNP1-2.0, Mountview Therapeutics, LLC) for 10 min, respectively. Then the nanoparticles were injected into mice via tail vein. 7 days later, mice were subjected to normoxia or hypoxia treatment.

2.6. NO detection

The culture medium NO level was detected using a Nitric Oxide Assay Kit (Abcam, ab65328) according to the manufacturer's protocols. Briefly, the nitrate was catalyzed with nitrate reductase into nitrite. Later, total nitrite was converted into a deep purple azo compound (azo chromophore) with Griess Reagents. The absorbance of the purple azo compound was measured at 540 nm, where the absorbance of the azo compound was directly proportional to NO production. The detection limit of the assay is approximately 1 nmol nitrite/well, or 10 μM.

2.7. Ca2+ flux measurement

Ca2+ flux in SMCs was imaged using fluorescence microscopy. Unless otherwise specified, cultures were incubated at room temperature for 45 min in the presence of Fluo-4 AM (10 μg/ml; F10489, Molecular Probes) and then de-esterified for 45 min.

2.8. Measurement of barrier function by trans endothelial electrical resistance (TEER)

Measurement of TEER on PAEC monolayers was used to determine the effect of TGF-β-induced EndoMT on barrier integrity and performed using the Epithelial Volt/Ohm (TEER) Meter, EVOM2 (World Precision Instruments, Sarasota, FL) as previously described [28]. In brief, PAECs were transfected with empty vector or PGC-1α expression plasmid. 2 days later, PAECs (1×10 [5]/well) were seeded on the upper chamber of a 24 well Transwell plate. The cells were allowed to form monolayers until stable TEER values were reached. Then, the monolayers were exposed to TGF-β (5 ng/ml, 240-B, R&D) for 3 days. The resistance was measured at 4000 Hz in 20 min intervals and normalized to the baseline level. Confluent PAEC monolayers showed the baseline TEER readings between 1000 and 2000 V. Data were shown as the percent changes relative to the baseline TEER ± SD from at least three independent experiments with three replicates each.

2.9. In vitro permeability assay

The In vitro permeability assay was performed as described previously with some modifications [29]. Briefly, we precoated Transwell inserts of 24-well plates (Corning Life Sciences, Tewksbury, MA) with gelatin. PAECs were transfected with empty vector or PGC-1α expression plasmids and then seeded (1×10^5 cells/well) on the upper chamber of a 24 well Transwell plate and cultured overnight or until confluency. The medium was then replaced with medium containing heparin binding growth factor and vascular endothelial growth factor. Fluorescein isothiocyanate (FITC)–BSA (0.5 mg/well, A9771-50 MG, Sigma) was added to the upper chamber. In the meantime, saline buffer was added to the lower chamber. The medium in the lower chamber was collected 6 h later and quantified for FITC signal with a fluorescence plate reader.

2.10. Flow cytometry

Following euthanasia and perfusion through the right ventricle with 5 ml of PBS, mouse lungs were removed, and the large airways were dissected to collect the peripheral lung tissues, which were cut into small pieces with scissors and transferred into tubes in which digestion buffer (1 mg/ml of collagenase D and 0.1 mg/ml DNase I, both from Roche, Indianapolis, IN, in Hanks' balanced salt solution) was added and incubated in 37 °C water bath for 30 min. Enzyme digested lungs were passed through 40-μm nylon mesh to obtain a single-cell suspension. Cells were centrifuged at 800 rpm/min for 5 min. After that, cells were resuspended with 1 ml PBS. Remaining red blood cells, if any exist, were

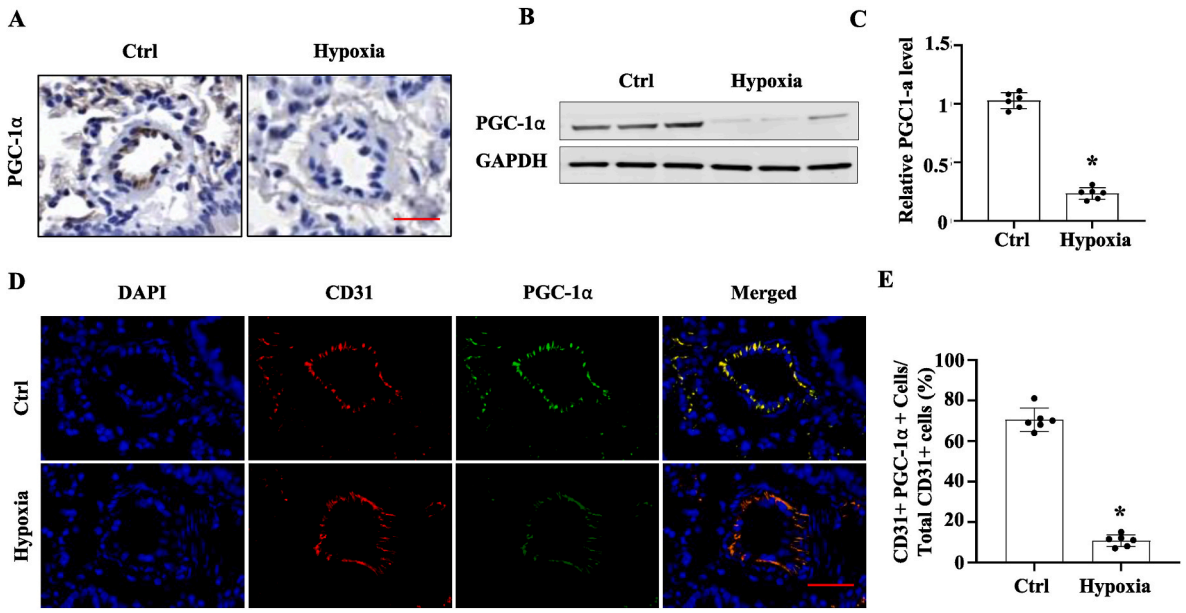

Fig. 1. PGC-1α expression was decreased in pulmonary artery endothelial cells in hypoxia-induced PAH mouse model. Wild-type (WT) mice were exposed to normoxia (n = 6) or hypoxia (10% O2, n = 6) for 4 weeks. **A**, Representative images of immunohistochemistry staining of PGC-1α in pulmonary arteries. Scale Bar: 100 μm. **B–C**, PGC-1α protein expression in the lung tissues, as detected by Western blot (B) and quantified by normalizing to GAPDH level. *p < 0.01 compared with the Control (Ctrl) group. **D**, PGC-1α expression in endothelial cells of normoxia (Ctrl) and hypoxia-treated lungs. Co-immunostaining of CD31 (red) with PGC-1α (green) was performed in mouse pulmonary arteries. Scale Bar: 100 μm. **E,** The percentage of PGC-1α + $CD31^+$ cells relative to the total $CD31^+$ cells as quantified from 10 sections of each artery. *p < 0.01 compared to the Ctrl group, n = 6. (For interpretation of the references to colour in this figure legend, the reader is referred to the Web version of this article.)

lysed using red blood cell lysis buffer (Roche, 11814389001, USA).

Cells were incubated with CD31 magnetic beads (11155D, ThermoFisher, USA). The captured cells were incubated with FcBlock (BD Biosciences, Cat # 564220) and stained with a mixture of FITC-conjugated CD31 antibody (Biolegand, Cat # 102405) and Rabbit anti-PGC-1α antibody (Cell Signaling, Cat# 2178) for 1 h. Cells were then washed with PBS for 3 times followed by incubation with Cy5-conjugated secondary anti-rabbit antibody. After washing with PBS for 3 times, cells were passed through a 70-μm filter and sorted on a BD FACSAria Fusion, BD Fortessa, or BD Canto II analyzer.

2.11. Measurement for pulse wave velocity (PWV)

Mouse anesthesia was induced with 3% isoflurane and maintained with 1.5% isoflurane. After shaving the chest, a depilatory cream (Nair; Carter-Horner, Mississauga, Ontario, Canada) was applied. Transthoracic closed-chest echocardiography was performed on 60 MHz (Vevo 1100, Visualsonics, Toronto, Canada) by following the procedure described previously [30]. Transthoracic 2-D, M-mode, and pulsed-wave Doppler Echo (Vevo 1100 ultrasound system, VisualSonics) were obtained with MS400 scan head. PWV is measured at two points along the pulmonary artery with one point in the tip of the pulmonary valve leaflets and one point in the main pulmonary artery. Briefly, the Pulsed-wave Doppler pointer was aligned to maximize laminar flow, and doppler tracings were recorded at a sweep speed of 400 mm/s. Blood velocity was recorded at these two points, and then the distance between these two points was measured using B-Mode. PWV is calculated as the separation distance divided by the pulse transit time between these two points (Vevo 1100 workstation).

2.12. Measurement of right ventricular to Left Ventricular Diameter Ratio at End-Systole

Mouse anesthesia was induced with 3% isoflurane and maintained with 1.5% isoflurane. The mouse heart rate and body temperature were monitored during the transthoracic echocardiography, which was performed using a Vevo 1100 system (VisualSonics, Toronto, ON, Canada) as described previously [31]. Ventricular to Left Ventricular Diameter Ratio at End-Systole (RV/LV + S) was calculated by evaluating the ratio of right ventricle (RV) weight to left ventricle (LV) plus inter-ventricular septum (S) weight (RV/LV + S).

2.13. In vivo permeability assay

To perform the vascular leakage assay in the PH mouse model, FITC-BSA (A9771-50 MG, sigma, USA) was injected (10 mg/ml) via the intravenous route 30 min before the mice were sacrificed. After euthanizing mice, 50 ml saline was used to perfuse the mice to remove remaining BSA in vessel. Then tissue was embedding with OCT and 5 μm sections were made by frozen sections.

2.14. Pulmonary artery pressure myography

Pressure myography was performed as described previously with some modifications [32,33]. Animals were euthanized by CO_2 inhalation followed by cervical dislocation. The heart and lungs were rapidly removed and placed into Krebs physiological saline solution (PSS: 118 mM NaCl, 24 mM $NaHCO_3$, 1 mM $MgSO_4$, 0.44 mM NaH_2PO_4, 4 mM KCl, 5.5 mM glucose and 1.8 mM $CaCl_2$). Small intrapulmonary arteries (third order branches, 80–200 μm in diameter) were dissected from connective and adipose tissues. The arteries were placed in ice-cold HEPES-PSS solution pre-equilibrated with 95% O_2 for 15 min. Glass cannulas in the pressure myograph chamber (DMT Model 110P) were filled with HEPES-PSS solution by a 10 ml syringe through inlet and outlet valves. Vessels were mounted on each end of the cannula and tied with 8-0 nylon suture. The intraluminal pressure was gradually increased via the P1 valve by selecting P1 pressure in the myo-interface panel manually or using software control. The pressure used for measurement were 5 → 10 → 20 → 40 → 60 → 80 → 100 → 120 mmHg. Vessels' diameters were recorded via the camera mounted above the

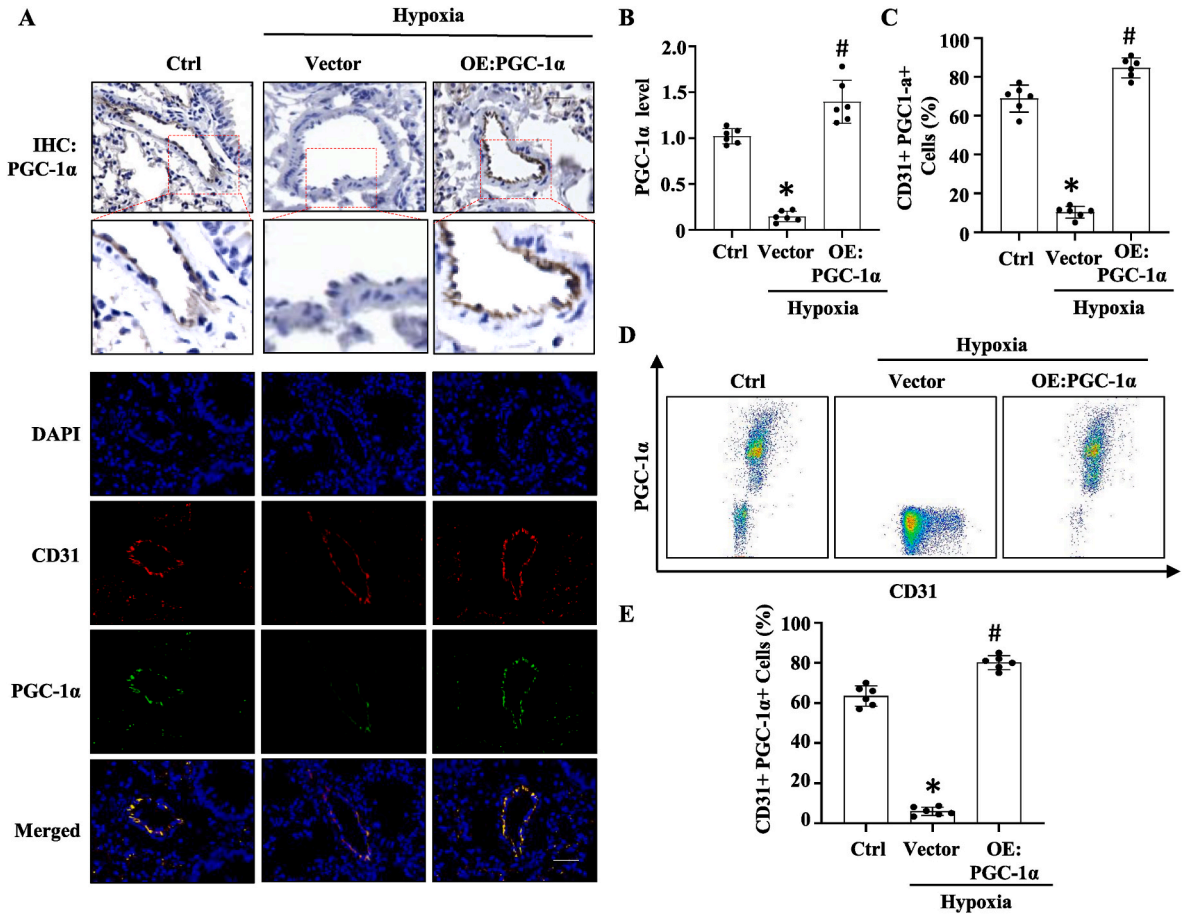

Fig. 2. PGC-1α overexpression in pulmonary artery endothelial cells via nanoparticle delivery in hypoxia-induced PAH mice. Nanoparticles containing empty vector or PGC-1α overexpression plasmid (OE: PGC-1α) was injected to mice via tail vein. After 7 days, mice were exposed to normoxia or hypoxia (10% O2) for 4 weeks. **A,** Immunohistochemistry (IHC) staining for PGC-1α (upper panel) and co-immunostaining of PGC-1α with CD31 (lower panels) of lung tissues. PGC-1α was downregulated in PAECs after hypoxia treatment. However, nanoparticle delivery of PGC-1α plasmid restored the PGC-1α expression. Scale bar: 100 μm. **B**, Relative PGC-1α levels in IHC staining as shown in A, as quantified by normalizing to the PGC-1α signal intensity in the normoxia group (Ctrl), which was set as 1. *P $<$ 0.01 vs. Ctrl; #P $<$ 0.01 vs. Vector group; n = 6. **C,** The percentage of PGC-1α+CD31$^+$ cells relative to the total CD31$^+$ cells, as quantified from 10 sections of each animals. **D-E,** Flow cytometry analyses. Lung tissues were digested, and PAECs were isolated by CD31 magnetic beads. Flow cytometry was performed to quantify PGC-1α+ PACEs (D), and the percentage of PGC-1α+ CD31$^+$ cells relative to the total CD31$^+$ cells was shown (E). *P $<$ 0.01 vs. Ctrl; #P $<$ 0.01 vs. Vector group; n = 6.

chamber.

2.15. Picrosirius red staining

Picrosirius red staining was performed using a commercial kit (ab150681, Abcam) following the manufactures' protocol. Briefly, staining was performed on tissue sections using 0.1% Sirius red in saturated picric acid at 25 °C for 1 h. Subsequently, sections were rinsed in 0.01 N HCl for 2 min. The sections were dehydrated in various concentrations of ethanol in the order of 70%, 80%, 95% and 100%, each for 10 s and then cleared in xylene twice, 10 min each. Sections were sealed with Xylene mounting medium (245–691, ThermoFisher, USA) and a glass cover slip.

2.16. Human IPAH samples

Human healthy and IPAH lung specimens were obtained from Mizzou Gift of Body Program, School of Medicine, University of Missouri. All samples were de-identified. The lung specimens were fixed overnight in formalin, embedded in paraffin, sectioned, and subsequently used for immunostaining. Lung proteins were extracted from formalin-fixed tissues by following the protocol published previously [34,35]. IPAH was determined via both medical history and pathological analyses.

2.17. Statistic analyses

All experiments were repeated at least for three times. All data represent independent data points but not technical replicates. Data are presented as the mean ± SD. Normality of data was assessed by the D'Agostino & Pearson normality test with alpha = 0.05. For comparisons of two groups, student's unpaired two-tailed *t*-test was used for normally distributed data, and Mann-Whitney two tailed test was used for non-normally distributed data or for groups with n less than 7. For more than 2 groups, 1-way ANOVA with Tukey post-test analysis was used for normally distributed data and Kruskal-Wallis test with Dunn's multiple comparisons test was used for non-normally distributed data. Prism 9.0 (GraphPad Software, CA) or RStudio (Desktop 1.4.1717) was used for statistical analyses, and differences considered statistically significant when nominal P $<$ 0.05 or adjusted P $<$ 0.05 in case of multiple testing.

3. Results

3.1. PGC-1α expression is decreased in PAECs in hypoxia-induced PH mouse model

To verify whether PGC-1α is involved in the development of PH, we

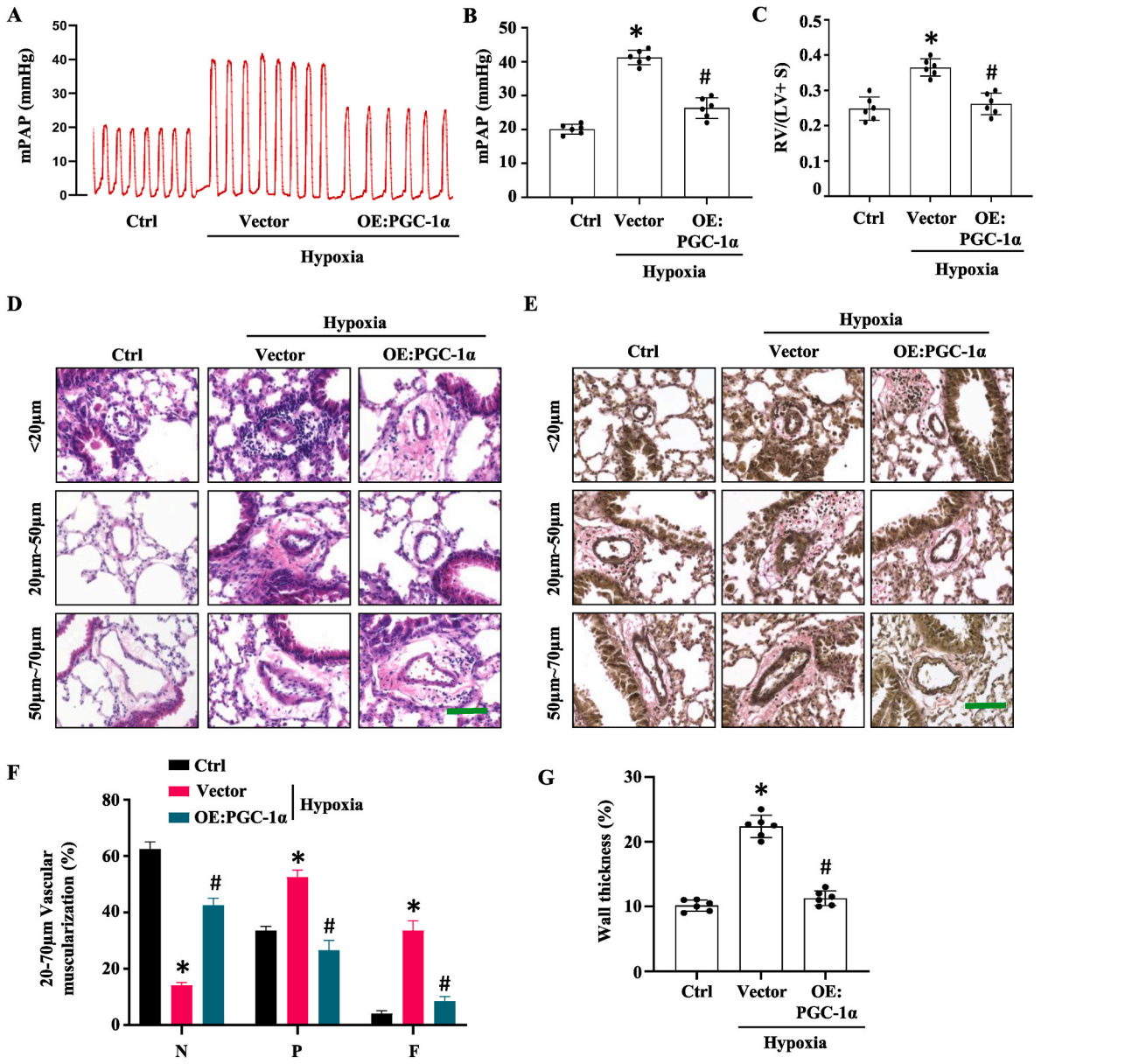

Fig. 3. Overexpression of PGC-1α in pulmonary artery endothelial cells ameliorated hypoxia-induced PAH and vascular remodeling in lungs. Nanoparticles containing control vector or PGC1-a overexpression plasmid (OE:PGC-1α) was injected to mice via tail vein. Mice were exposed to normoxia or hypoxia (10% O2) for 4 weeks. **A-B**, Assessment of mean pulmonary aorta pressure (mPAP). *P < 0.01 vs. Ctrl; #P < 0.01 vs. Vector group; n = 6. **C**, Ratio of right ventricle to left ventricle + septum weight [RV/(LV + S)]. *P < 0.01 vs. Ctrl; #P < 0.01 vs. Vector group; n = 6. **D-E**, H &E (D) and elastic van Gieson staining (E) of the pulmonary arteries. Artery wall thickening of pulmonary arteries with different diameters are shown. Scale Bar: 100 μm. **F**, Quantification of pulmonary arterial muscularization in arteries with diameters 20–70 μm. N = non-muscularized vessels; P = partially muscularized vessels. F = fully muscularized vessels. *P < 0.01 vs. Ctrl; #P < 0.01 vs. the vector group for each vessel type, respectively; n = 6. G, Quantitative assessment of the wall thickness of the pulmonary arteries as described in Methods. *P < 0.01 vs. Ctrl; #P < 0.01 vs. Vector group; n = 6.

first used a hypoxia-induced PH mouse model by exposing C57BL6 mice to normoxia or hypoxia (10% O_2) for 4 weeks. The immunohistochemistry staining showed that PGC-1α is downregulated in PH lungs as compared with the normal controls (Fig. 1A). Western blotting showed that PGC-1α expression was significantly blocked in PH lungs due to the hypoxia treatment (Fig. 1, B–C). Interestingly, the majority of PGC-1α was expressed in the lung endothelium of the normoxia-treated mice, which was diminished in PH lungs. To confirm if PGC-1α is mainly expressed in endothelial cells, we co-stained endothelial cell marker CD31 with PGC-1α in the normal and PH lungs. As shown in Fig. 1, D-E, PGC-1α was expressed in 64.3% of the PAECs in the normal control lungs (64.3%), but, only 10% of PAECs expressed PGC-1α in the PH lungs. Moreover, the intensity of PGC-1α staining was also dropped in PH lungs as compared to the control lungs (Fig. 1D). These results suggest that PGC-1α downregulation in PAECs may contribute to the development of PH.

3.2. *Overexpression of PGC-1α specifically in PAECs via nanoparticle delivery of Cdh5 promoter-driven PGC-1α plasmid*

In order to determine the role of PGC-1α in PH, we constructed an endothelial-specific PGC-1α expression plasmid, driven by endothelial specific promoter Cdh5. The control vector and PGC-1α plasmids were packaged individually into poly (ethylene glycol) methyl ether-block-poly (lactide-coglycolide) (PEG-b-PLGA) copolymer-based nanoparticles formulated with polyethyleneimine [27]. The mixture of

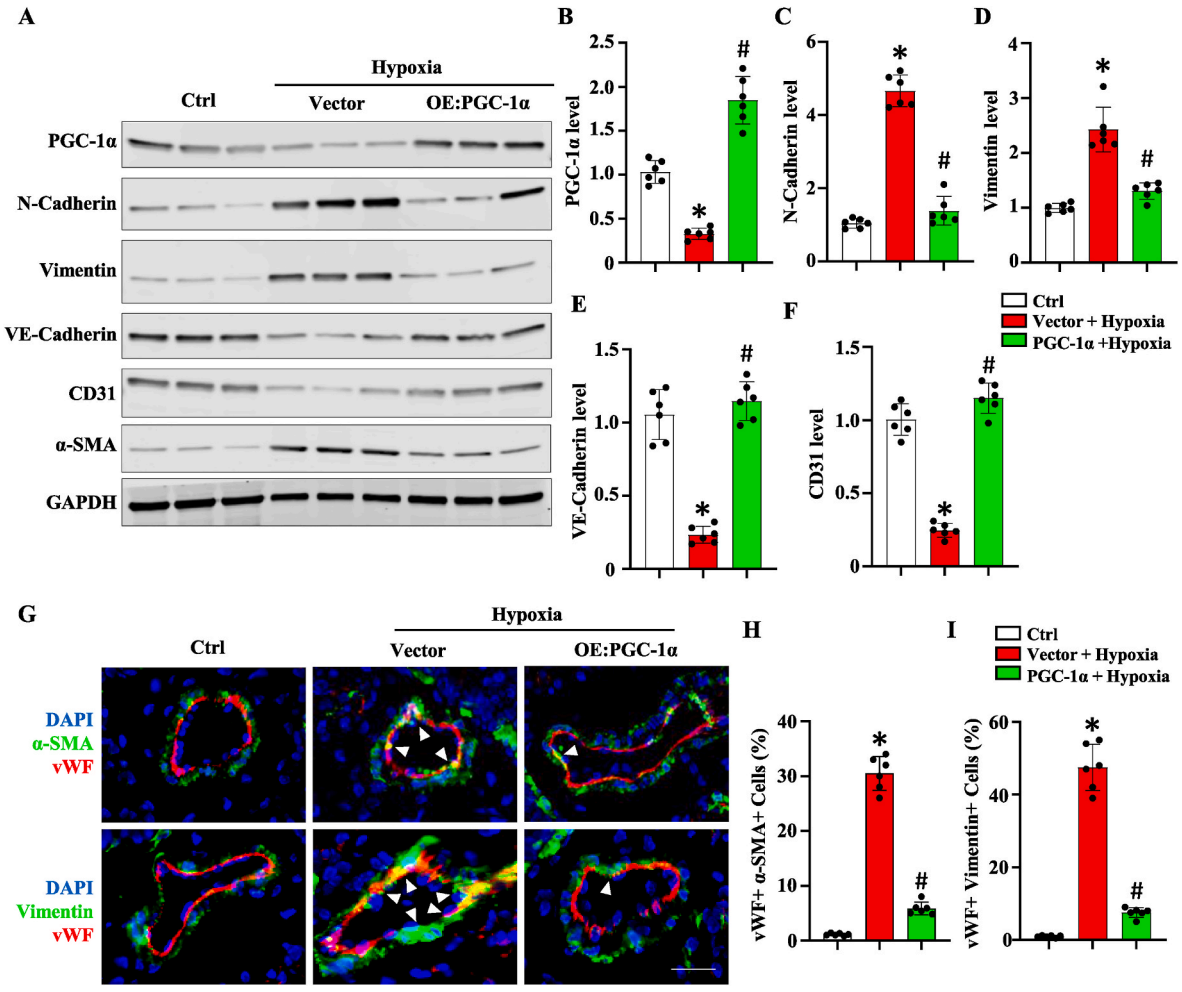

Fig. 4. PGC-1α overexpression attenuated hypoxia-induced endothelial-mesenchymal transition *in vivo*. Nanoparticles containing control vector (WT) or PGC-1α expression plasmid (OE:PGC1-a) were injected to mice via tail vein. Mice were exposed to normoxia (Ctrl) or hypoxia (10% O2) for 4 weeks. **A,** PGC-1α, mesenchymal markers N-Cadherin and vimentin, and endothelial cell markers VE-Cadherin and CD31 protein expression levels in the lung tissues, as detected by Western blotting. **B–F**, Quantification of PGC-1α (B), N-Cadherin (C), vimentin (D), VE-Cadherin (E) and CD31 (F) protein levels by normalizing to GAPDH, respectively. Shown are fold changes relative to the normoxia group. *P < 0.01 vs. Ctrl; #P < 0.01 vs. Vector group for each individual proteins, respectively; n = 6. **G**, Co-immunostaining of vWF with α-SMA or Vimentin in lung tissues. vWF co-localized with α-SMA and Vimentin in PAECs after hypoxia treatment (white arrowheads), which was diminished by nanoparticle delivery of PGC-1α. Scale bar: 40 μm. **H–I**, The percentage of vWF+ α-SMA + cells (H) and vWF + Vimentin + cells (I) relative to the total vWF + cells, as quantified from 10 sections of each lung arteries. *P < 0.01 vs. Ctrl; #P < 0.01 vs. Vector-treated group, n = 6.

nanoparticles and plasmid DNA was administered into mice via tail vein. Mice were then exposed to either normoxia or hypoxia (10% O_2) for 4 weeks. To determine the efficiency of PGC-1α expression, immunohistochemistry staining was performed on lung tissue sections using PGC-1α antibody. Consistent with data shown in Fig. 1A, PGC-1α was dramatically downregulated in PH lungs. However, PGC-1α plasmid delivery restored the expression of PGC-1α in endothelium of mice treated with hypoxia (Fig. 2, A–B). In fact, the PGC-1α levels in PGC-1α plasmid-delivered lungs were higher than the normal control lungs. To determine if PGC-1α plasmids were mainly delivered to and expressed in PAECs, we co-stained CD31 with PGC-1α in the control and hypoxia-treated lungs with or without PGC-1α plasmids, and found that PGC-1α plasmid specifically overexpressed PGC-1α in PAECs of the lungs with hypoxia (Fig. 2, A–C). To further verify the overexpression of PGC-1α in endothelial cells, we prepared single cell solution of lung tissues using enzyme digestion cocktail as described in methods, and then PAECs were isolated by using CD31 magnetic beads. Flow cytometry analyses demonstrated that PGC-1α was expressed in the majority of PAECs in hypoxia-treated lungs (Fig. 2, D-E). These results showed that PGC-1α expression plasmid successfully restored the expression of PGC-1α in hypoxia-treated mouse lungs.

3.3. Overexpression of PGC-1α in PAECs ameliorates hypoxia-induced PH and vascular remodeling in mouse lungs

To determine if PGC-1α can block the development of PH, mice with nanoparticle delivery of control or PGC-1α expression plasmid were exposed to normoxia or hypoxia (10% O_2) for 4 weeks. We found that right ventricular systolic pressure (RVSP) was dramatically increased in hypoxia-treated mice. However, PGC-1α overexpression suppressed the elevation of RVSP from 40 mmHg to 23 mmHg (Fig. 3, A–B). These data indicated that overexpression of PGC-1α ameliorates hypoxia-induced PH in mice. Increased RVSP lead to right ventricle (RV) hypertrophy, which can be evaluated by the ratio of RV weight to left ventricle (LV) plus inter-ventricular septum (S) weight (RV/LV + S). Hypoxia-treated mice exhibited a significant increase in the RV/(LV + S) ratio as compared to the normoxia controls (Fig. 3C). But the maladaptive changes were blocked in mice with PGC-1α overexpression in PAECs (Fig. 3C). These results indicate that endothelial overexpression of PGC-1α protects mice from RV hypertrophy in hypoxia-induced PH model.

Pulmonary vascular remodeling is a hallmark of PH. We thus determined the numbers and the wall thickness of α-SMA + arteries ranging from 20 to 70 μm in diameter according to the criteria described

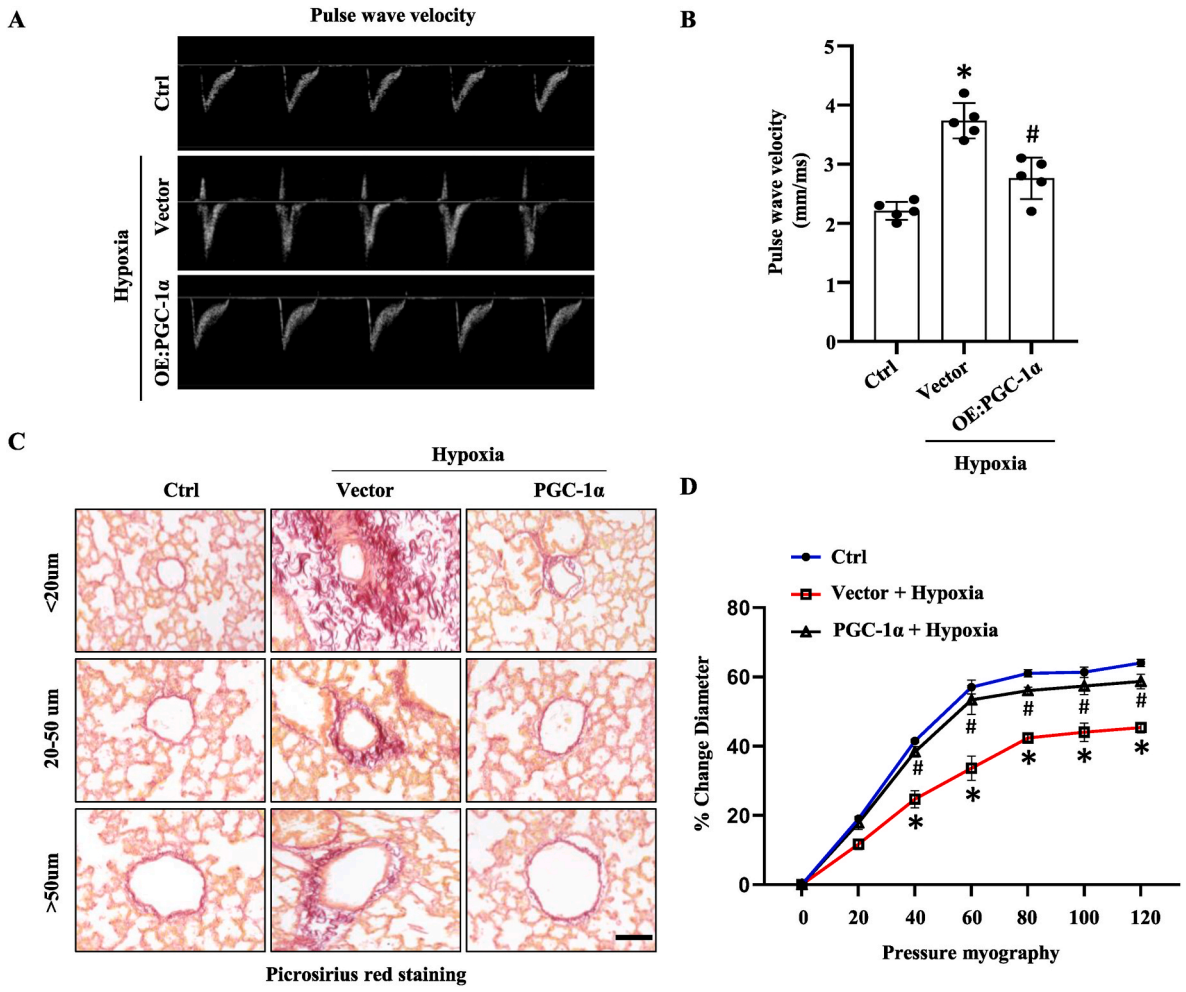

Fig. 5. Overexpression of PGC-1α reduced pulmonary artery stiffness. Nanoparticles containing empty vector and PGC-1α expression plasmid (OE:PGC1-a) were injected to mice via tail vein. Mice were exposed to normoxia (Ctrl) or hypoxia (10% O2) for 4 weeks. **A**, The pulse-wave Doppler recordings. The pulse wave velocity (PWV) was increased in hypoxia-treated mouse pulmonary arteries, which was attenuated by endothelial overexpression of PGC-1α. **B**, PWVs were shown as millimeter/millisecond. *P < 0.01 vs. Ctrl; #P < 0.01 vs. Vector group; n = 5. **C,** Picrosirius red staining of pulmonary arteries with various diameters as indicated. Scale Bar: 100 μm **D**, Artery distensibility measurement. The pulmonary arteries from the left lobe of 7-8-week old male mice were isolated, and third order branches (<200 μm) were selected for pressure myography. The diameter alterations under the indicated pressures were recorded. *P < 0.01 vs. Ctrl; #P < 0.01 vs. Vector group with each individual pressure; n = 6. (For interpretation of the references to colour in this figure legend, the reader is referred to the Web version of this article.)

previously [36]. Our data showed that endothelial overexpression of PGC-1α significantly attenuated pulmonary vascular remodeling in hypoxia-induced PH mouse model (Fig. 3, D–G). Both Elastin van Gieson and H&E staining (Fig. 3, D-E) exhibited that the significant increase in pulmonary artery muscularization and wall thickening observed in hypoxia-treated mouse lungs were alleviated by endothelial PGC-1α overexpression. Together, these results demonstrated that endothelial overexpression of PGC-1α ameliorates hypoxia-induced PH, vascular remodeling in lungs, as well as RV hypertrophy.

3.4. *PGC-1α overexpression attenuates hypoxia-induced EndoMT in vivo*

EndoMT plays an important role in the development and progression of pulmonary hypertension. EndoMT is a process by which ECs lose their cobblestone morphology and characteristic gene expression and gain phenotypic features and expression of genes commonly associated with SMCs and fibroblasts/myofibroblasts. At the molecular level, EndoMT results in progressive loss of endothelial markers CD31 and VE-cadherin, while gaining mesenchymal markers vimentin, N-Cadherin, and α-SMA. PGC-1α has been reported to participate in the regulation of EndoMT. To determine if PGC-1α attenuates PH development via regulating EndoMT, we detected the protein expression of PGC-1α, N-Cadherin, Vimentin, VE-Cadherin, CD31, and α-SMA in mouse lung tissues and found that mesenchymal markers vimentin, N-Cadherin, and α-SMA expression was increased with loss of endothelial markers CD31 and VE-cadherin in mice with control vector nanoparticle delivery under hypoxia treatment. However, endothelial overexpression of PGC-1α suppressed the expression of mesenchymal markers while restored the expression of endothelial markers (Fig. 4, A–F), indicating that PGC-1α blocks EndoMT in PH lungs. To verify if EndoMT of PAECs occurs in our mouse PH model and if PGC-1α attenuates the EndoMT in pulmonary arteries, we co-stained endothelial cell marker Von Willebrand factor (vWF) with α-SMA and Vimentin, respectively, in the normal and hypoxia-treated mouse lungs. As shown in Fig. 4, G-I, α-SMA and Vimentin were expressed in 30.13% and 46.32% of vWF + cells, respectively, demonstrating that hypoxia treatment induced EndoMT of PAECs in PH mouse lungs. However, only 8.11% and 9.94% of PAECs were observed to express α-SMA and Vimentin, respectively, in PGC-1α-overexpressed mouse lungs under hypoxia treatment. These results indicated that EndoMT of PAECs is a critical process contributing to the PH development, and PGC-1α blocks PH by impeding the EndoMT of PAECs.

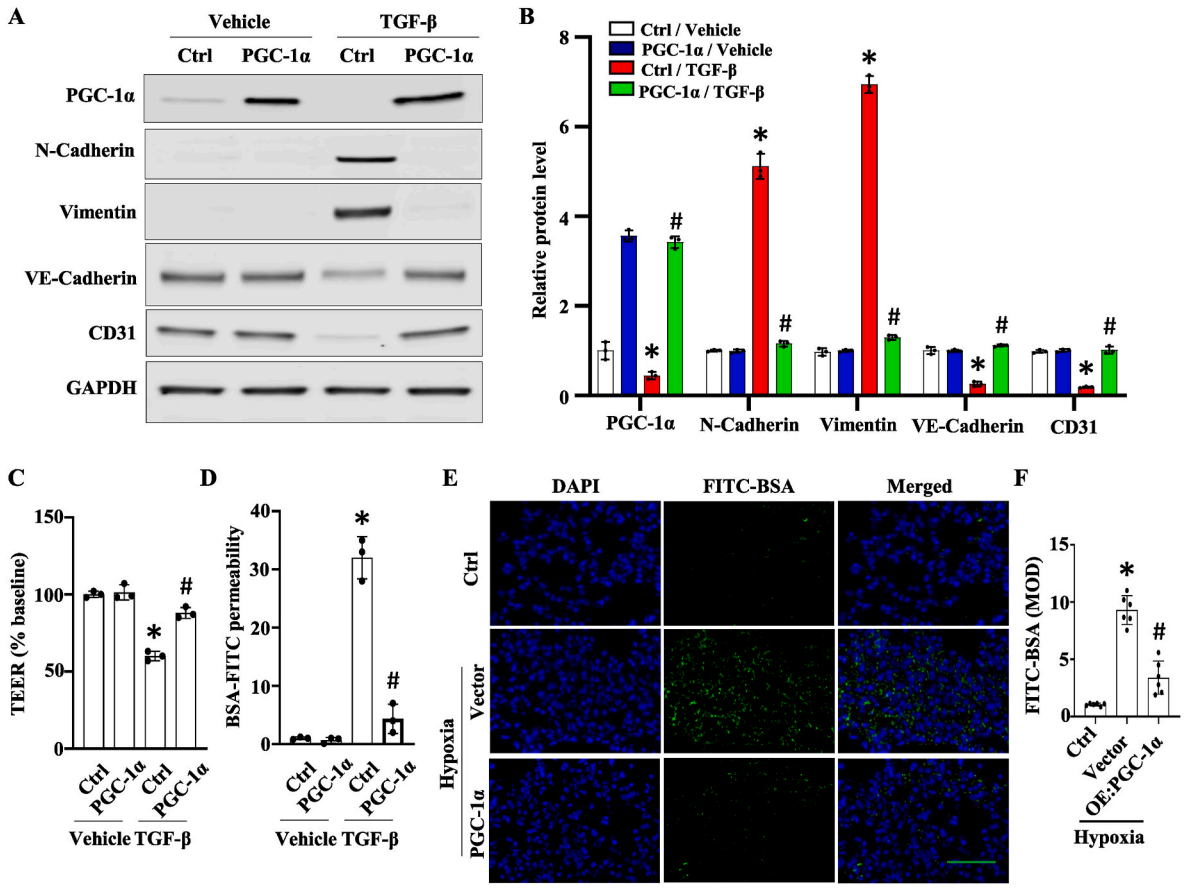

Fig. 6. Overexpression of PGC-1α attenuated TGF-β-induced EndoMT and disruption of endothelial monolayer integrity. Human pulmonary artery endothelial cells (PAECs) were transfected with empty vector (Ctrl) or PGC-1α expression plasmid and then treated with vehicle or TGF-β (5 ng/ml) for 3 days. **A-B**, PGC-1α, N-Cadherin, Vimentin, VE-Cadherin, CD31 protein expression, as detected by Western blotting (A) and quantified by normalizing to GAPDH (B), respectively. *P < 0.05 vs. vehicle-treated cells; #P < 0.01 vs. Ctrl vector-transfected cells with TGF-β for each individual proteins; n = 3. **C,** *Trans*-Endothelial Electrical Resistance (TEER) measurement. TEER was measured continuously in PAECs with or without TGF-β treatment. After baseline TEER was achieved, TGF-β were added. 3 days later, the resistance was measured at 4000 Hz in 20 min intervals and normalized to the baseline level. *P < 0.05 vs. vehicle-treated cells; #P < 0.05 vs. Ctrl vector-transfected cells with TGF-β; n = 3. **D,** PAEC permeability assay. PAECs were plated on Transwell inserts and cultured until confluence. Vehicle or PBS along with fluorescein isothiocyanate (FITC)-dextran was added to the bottom chamber and incubated for 3 days. FITC-dextran leaked to the upper chamber was quantified by measuring the green fluorescent signals in a fluorescence plate reader. *P < 0.05 vs. vehicle-treated cells; #P < 0.05 vs. Ctrl vector-transfected cells with TGF-β; n = 3. **E**, *In vivo* permeability assay. Nanoparticles containing control vector (Ctrl) or PGC-1α expression vector (PGC-1α) were injected to mice via tail vein. Mice were exposed to normoxia or hypoxia (10% O2) for 4 weeks, and were then injected i.v. with FITC-BSA. 3 h later, animals were sacrificed and perfused with 4% paraformaldehyde (PFA). PAEC permeability was assessed by imaging the green fluorescent signals from leaked FITC-BSA with a fluorescence microscope (E) and quantified by normalizing to the fluorescent signals in normoxia-treated group, which was set as 1 (F). Scale Bar: 100 μm *P < 0.01 vs. Ctrl; #P < 0.01 vs. Vector group; n = 6. (For interpretation of the references to colour in this figure legend, the reader is referred to the Web version of this article.)

3.5. *Overexpression of PGC-1α reduces pulmonary artery stiffness*

EndoMT-generated myofibroblasts cause increased production of extracellular matrix proteins, which reduce artery compliance due to the vascular remodeling. In order to determine if PGC-1α is beneficial for pulmonary artery compliance, we examined pulmonary artery stiffness, the inverse of arterial compliance, by measuring the artery pulse wave velocity (PWV). As shown in Fig. 5, A-B, the PWV in pulmonary arteries of hypoxia-treated mice were significantly increased compared to the mice with normoxia treatment. However, endothelial overexpression of PGC-1α significantly decreased the PWV, suggesting that PGC-1α can restore pulmonary artery compliance. Structurally, arterial stiffness or reduced compliance is due to increased collagen deposition in artery wall. Indeed, Picrosirius Red staining showed that hypoxia treatment dramatically increased collagen deposition around pulmonary arteries in mice with nanoparticle delivery of control vector. However, endothelial overexpression of PGC-1α diminished the collagen accumulation (Fig. 5C), at least partially due to the blockade of EndoMT of PAECs in these arteries. To directly measure pulmonary artery compliance, the third order branches of pulmonary arteries (<200 μm) from the left lobe of 7–8 weeks old mice were isolated and mounted for pressure myography to record their diameters under various pressures. As shown in Fig. 5D, hypoxia-treated pulmonary arteries exhibited significantly reduced compliance as shown by the increased arterial stiffness. However, endothelial overexpression of PGC-1α restored the artery compliance as revealed by the significantly increased expansion of artery diameters under different pressures compared to the arteries with control vector delivery. These data demonstrated that endothelial overexpression of PGC-1α restores pulmonary artery compliance by reducing the artery stiffness.

3.6. *Overexpression of PGC-1α reverses EndoMT and protects endothelial integrity*

To directly test whether PGC-1α mediates PAEC EndoMT, we treated human PAECs with TGF-β and found that TGF-β significantly down-regulated PGC-1α expression along with the induction of EndoMT as evidenced by the increased N-cadherin and vimentin expression and

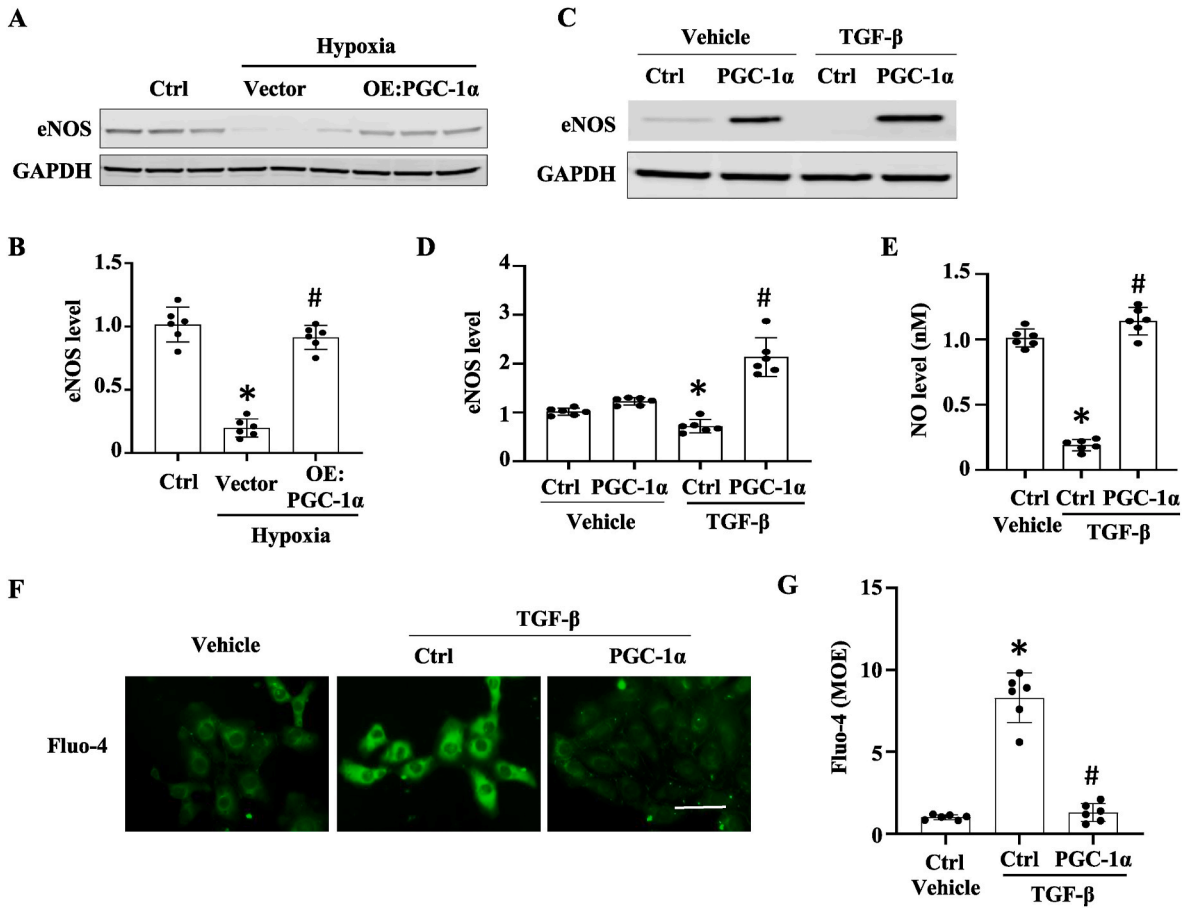

Fig. 7. Overexpression of PGC-1α improved PAEC function and inhibits calcium release in smooth muscle cells (SMCs). Nanoparticles containing control vector or PGC1-α expression plasmid (OE:PGC1-α) were injected to mice via tail vein. Mice were exposed to normoxia (Ctrl) or hypoxia (10% O2) for 4 weeks. **A-B**, Endothelial nitric oxide synthase (eNOS) expression in lung tissues, as detected by Western blotting (A) and normalized to GAPDH. *P < 0.01 vs. Ctrl; #P < 0.01 vs. Vector group; n = 6. **C-D**, eNOS protein expression. Human PAECs were transfected with empty vector (Ctrl) or PGC-1α expression plasmid and then treated with vehicle or TGF-β (5 ng/ml) for 3 days. eNOS expression was detected by Western blotting (C) and normalized to GAPDH (D). *P < 0.05 vs. vehicle-treated cells; #P < 0.01 vs. Ctrl vector-transfected cells with TGF-β; n = 6. **E,** Nitric oxide (NO) release assay. PAECs were treated with nanoparticles containing empty Vector (Ctrl) or PGC-1α expression plasmid (PGC-1α). One day later, cells were treated with vehicle or TGF-β for 20 min. NO generated by PAECs was measured using a Nitric Oxide Assay Kit (Abcam, ab65327). The relative NO levels were quantified by normalizing to the vehicle-treated cells, which was set as 1. *P < 0.01 vs. vehicle-treated cells; #P < 0.01 vs. Ctrl vector nanoparticle-treated cells with TGF-β; n = 6. **F-G**, Calcium flux assay. PAECs were transfected with empty vector (Ctrl) or PGC-1α expression plasmid and cocultured with SMCs in a transwell plate. PACEs in the upper chamber were treated with vehicle (Ctrl) or TGF-β (5 ng/ml) for 3 days. Then SMCs in the lower chamber were incubated with Fluo-4 AM at 37 °C and room temperature each for 45 min. Calcium flux signal (green) was detected with a Nikon fluorescence microscope using FITC channel (F) and normalized to control (G). *P < 0.05 vs. vehicle-treated cells; #P < 0.01 vs. Ctrl vector-transfected cells with TGF-β; n = 6. (For interpretation of the references to colour in this figure legend, the reader is referred to the Web version of this article.)

decreased VE-cadherin and CD31 expression (Fig. 6, A–B). However, overexpression of PGC-1α restored the expression of endothelial markers while suppressed the expression of mesenchymal cell markers (Fig. 6, A-B).

Emerging evidences show that EndoMT disrupts endothelial integrity, which further increased EC permeability. Thus, we tested the PAEC integrity by measuring transepithelial electrical resistance (TEER), a widely accepted quantitative technique to measure the integrity of tight junction dynamics in cultured ECs, and performed FITC-BSA permeability assay. As shown in Fig. 6C, TGF-β treatment of PAECs resulted in a significant reduction of TEER, indicative of the disruption of endothelial tight junction. However, overexpression of PGC-1α restored the TGF-β-reduced TEER (Fig. 6C). FITC-BSA permeability assay showed that overexpression of PGC-1α blocked TGF-β treatment-caused drastic increase in PAEC permeability (Fig. 6D). These data demonstrated that PGC-1α is able to protect the PAEC integrity.

To determine if PGC-1α affects PAEC permeability *in vivo*, FITC-BSA was administered via tail vein injection into mice with endothelial-specific delivery of control or PGC-1α expression plasmid 2 h before euthanasia and saline perfusion. As shown in Fig. 6, E-F, hypoxia treatment caused significant amounts of FITC-BSA to leak out into mouse lung tissues, suggesting a dramatic increase in EC permeability in pulmonary arteries. However, much less FITC-BSA leakage was observed in the lungs with endothelial overexpression of PGC-1α (Fig. 6, E-F). These results indicated that PGC-1α-attenuated EndoMT protects endothelial integrity by decreasing EC permeability *in vivo*.

3.7. Overexpression of PGC-1α improves PAEC function and inhibits calcium release in SMCs

Hypoxia-induced EndoMT not only affects endothelial integrity but also causes EC dysfunction. Indeed, hypoxia caused significant reduction of eNOS production in mouse lungs with control vector delivery. Endothelial-specific overexpression of PGC-1α, however, restored the eNOS expression (Fig. 7, A–B). To directly test the impact of PGC-1α on eNOS expression, we treated PAECs with TGF-β to induce EndoMT and found that TGF-β treatment caused a downregulation of eNOS, which was restored by the overexpression of PGC-1α in PAECs (Fig. 7, C-D).

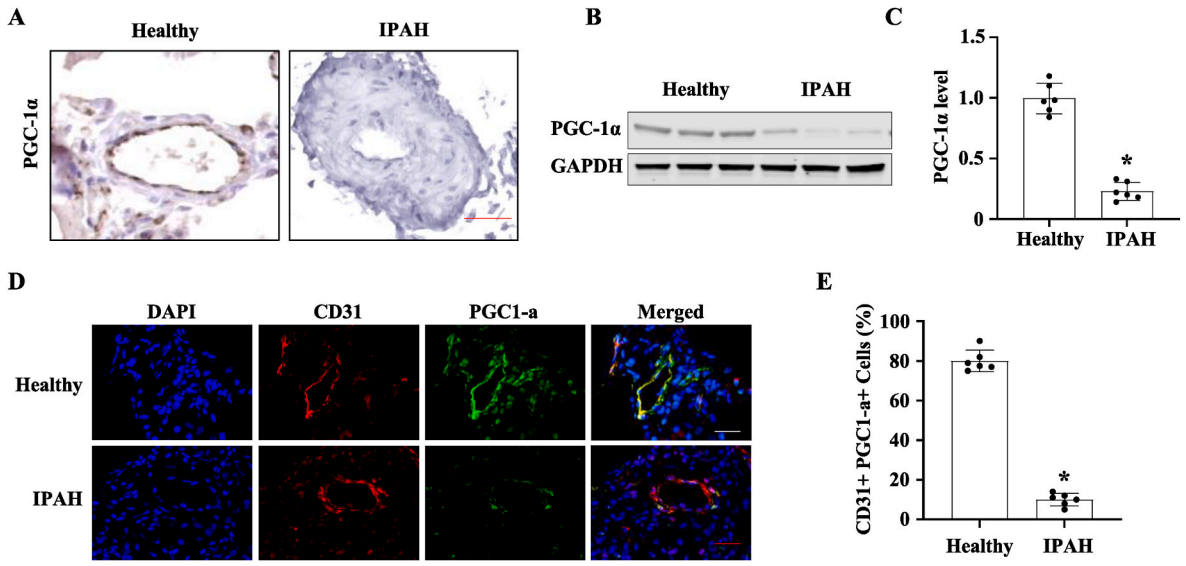

Fig. 8. PGC-1α was decreased in pulmonary artery endothelial cells of patients with idiopathic pulmonary arterial hypertension (IPAH). A, Representative images of immunohistochemistry staining of PGC-1α in pulmonary arteries. Scale Bar: 200 μm. **B–C,** PGC-1α protein expression in healthy and IPAH lungs, as detected by Western blotting (B) and quantified by normalizing to GAPDH level (C). *P < 0.01 vs. Healthy lungs, n = 6. **D,** PGC-1α expression in human pulmonary artery endothelium, as detected by co-immunostaining of PGC-1α (green) with CD31 (red) in lung tissues. Scale Bar: 100 μm. **E**, The percentages of PGC-1α+ $CD31^+$ cells relative to the total $CD31^+$ cells, which was quantified from 10 sections of each patients. *P < 0.01 vs. Healthy lungs, n = 6. (For interpretation of the references to colour in this figure legend, the reader is referred to the Web version of this article.)

Consistently, TGF-β treatment significantly reduced the NO production and release from PAECs, but PGC-1α boosted the NO production to the normal levels. These results clearly showed that PGC-1α can protect PAECs from EndoMT-caused EC dysfunction.

Since reduction in NO production due to EC dysfunction affects SMC relaxation, which further disturb artery compliance, we tested if endothelial-specific delivery of PGC-1α regulates SMC calcium flux. An increase in Ca^{2+} flux initiates SMC contraction in the process known as excitation–contraction coupling. To test this, human PAECs and SMCs were co-cultured in a Transwell plate. PACEs in upper chamber were treated with vehicle or TGF-β for 3 days. Then SMCs cultured in the lower chamber were incubated with Fluo-4 AM, a calcium indicator. TGF-β treatment of PAECs triggered a significant increase in calcium release in SMCs. But the calcium signal was diminished in SMCs cocultured with PGC-1α-overexpressed PAECs (Fig. 7, F-G). These results indirectly demonstrated that overexpression of PGC-1α in PAECs can restore SMC relaxation by resuming PAEC function in producing and releasing NO to SMCs.

3.8. PGC-1α is decreased in PAECs of patients with idiopathic PAH (IPAH)

To determine whether PGC-1α is involved in the development of human PAH, we detected PGC-1α expression levels in lung tissues from IPAH patients and normal controls. PGC-1α was highly expressed in lung vessels in the healthy human lungs, but it was dramatically downregulated in lung vessels, especially in the endothelium of PAH patients (Fig. 8A). Decreased expression of PGC-1α was further confirmed by Western blotting (Fig. 8, B–C). To determine if PGC-1α is mainly expressed in PAECs in human with IPAH, we co-immunostained PGC-1α with CD31 in human lung sections and found that the majority of PGC-1α was presented in $CD31^+$ PAECs (Fig. 8, D–E). The $CD31^+$ PGC-1α+ cells were significantly decreased in IPAH lungs (Fig. 8, D-E). These data suggest that PGC-1α could also protect the PAEC integrity in human lungs and thus impede the development of PAH in human patients.

4. Discussion

By using a hypoxia-induced PH mouse model, we found that PGC-1α is an important novel factor blocking the development of PH. PGC-1α is downregulated in both mouse and human PAECs during the PH development. However, endothelial-specific overexpression of PGC-1α significantly hinders the progression of PH, as shown by the significantly decreased RVSP, reduced artery thickness, and lessened vascular muscularization. Moreover, endothelial-specific overexpression of PGC-1α blocks the EndoMT of PAECs during PH, indicating that the loss of PGC-1α contributes to the PH development due, at least partially, to the EndoMT of PAECs.

Endothelial dysfunction is a contributing factor to vascular remodeling in PH [37], and EndoMT causes endothelial dysfunction [38]. EndoMT is a dynamic process in which ECs loss their endothelial properties and take on mesenchymal cell behaviors. The loss of junction proteins such as VE-cadherin also results in loosened adherens junctions, which in turn increases vascular permeability and enhances leukocyte trafficking, and consequently worsens the pulmonary vascular remodeling and PH progression. PGC-1α appears to be a potent factor blocking the EndoMT of PAECs, as evidenced by the restoration of endothelial marker proteins both *in vitro* and *in vivo*. Moreover, PGC-1α overexpression in ECs blocks EndoMT-disrupted EC integrity and further the increased permeability.

Inhalation of NO is an effective treatment for PH in term and near-term infants [39]. Nitric oxide signaling is important for maintaining vascular homeostasis and inhibiting the development of PH. eNOS generates the basal level of NO in ECs, which activates soluble guanylate cyclase and leads to cGMP production and subsequent activation of cGMP-dependent protein kinase G in SMCs. The activated protein kinase G causes SMC relaxation and inhibits pulmonary SMC proliferation, leading to reduced pulmonary vascular remodeling and thereby preserving normal pulmonary tension [40]. Decreased NO bioavailability leading to impaired protein kinase G activity is a common feature of PH [41]. Thus, current therapeutics focus on either downstream of NO pathway or inhaled NO itself. Our results provide a novel approach to increase NO bioavailability by addressing the underlying issues causing the reduction of NO levels in PH patients, i.e., endothelial

overexpression of PGC-1α restores NO level by reversing the EndoMT of PAECs and thus the EndoMT-caused PAEC dysfunction and pulmonary vascular remodeling, as shown by the effect of PGC-1α in reducing pulmonary artery stiffness and SMC calcium flux.

Taken together, our studies demonstrate that overexpression of PGC-1α in PAECs impedes PH development by blocking EndoMT of PAECs and preserving the integrity of pulmonary endothelium. As a result, PGC-1α reduces pulmonary artery stiffness by inhibiting pulmonary artery remodeling while enhancing eNOS expression and NO production in PAECs, which maintains the overall pulmonary homeostasis. These combined beneficial effects make PGC-1α as a potentially effective agent for developing therapeutics to hinder PH development.

Funding

This work was supported by the National Institutes of Health (HL123302, HL119053, HL135854, and HL147313); the University of Missouri School of Medicine, Columbia, MO (TRIUMPH Initiative Funding); and American Heart Association (657293 Postdoctoral Fellowship to D.C.).

Declaration of competing interest

None.

Data availability

Data will be made available on request.

Acknowledgements

We thank Dr. Youyang Zhao for providing the pGL3CDH5p-eGFP vector.

References

[1] K.Y. Chang, S. Duval, D.B. Badesch, T.M. Bull, M.M. Chakinala, T. De Marco, R. P. Frantz, A. Hemnes, S.C. Mathai, E.B. Rosenzweig, J.J. Ryan, T. Thenappan, P.I. *, Mortality in pulmonary arterial hypertension in the modern era: early insights from the pulmonary hypertension association registry, J. Am. Heart Assoc. 11 (2022), e024969.

[2] H.W. Farber, J. Loscalzo, Pulmonary arterial hypertension, N. Engl. J. Med. 351 (2004) 1655–1665.

[3] R.M. Tuder, E. Stacher, J. Robinson, R. Kumar, B.B. Graham, Pathology of pulmonary hypertension, Clin. Chest Med. 34 (2013) 639–650.

[4] P. Dorfmuller, Pulmonary hypertension: pathology, Handb. Exp. Pharmacol. 218 (2013) 59–75.

[5] H.A. Tuchscherer, E.B. Webster, N.C. Chesler, Pulmonary vascular resistance and impedance in isolated mouse lungs: effects of pulmonary emboli, Ann. Biomed. Eng. 34 (2006) 660–668.

[6] R.M. Tuder, How do we measure pathology in PAH (lung and RV) and what does it tell us about the disease, Drug Discov. Today 19 (2014) 1257–1263.

[7] B. Ranchoux, L.D. Harvey, R.J. Ayon, A. Babicheva, S. Bonnet, S.Y. Chan, J. X. Yuan, V.J. Perez, Endothelial dysfunction in pulmonary arterial hypertension: an evolving landscape (2017 Grover Conference Series), Pulm. Circ. 8 (2018), 2045893217752912.

[8] B. Ranchoux, F. Antigny, C. Rucker-Martin, A. Hautefort, C. Péchoux, H.J. Bogaard, P. Dorfmüller, S. Remy, F. Lecerf, S. Planté, S. Chat, E. Fadel, A. Houssaini, I. Anegon, S. Adnot, G. Simonneau, M. Humbert, S. Cohen-Kaminsky, F. Perros, Endothelial-to-mesenchymal transition in pulmonary hypertension, Circulation 131 (2015) 1006–1018.

[9] E. Yun, Y. Kook, K.H. Yoo, K.I. Kim, M.S. Lee, J. Kim, A. Lee, Endothelial to mesenchymal transition in pulmonary vascular diseases, Biomedicines 8 (2020).

[10] F. de la Cuesta, I. Passalacqua, J. Rodor, R. Bhushan, L. Denby, A.H. Baker, Extracellular vesicle cross-talk between pulmonary artery smooth muscle cells and endothelium during excessive TGF-beta signalling: implications for PAH vascular remodelling, Cell Commun. Signal. 17 (2019) 143.

[11] N. Rol, K.B. Kurakula, C. Happe, H.J. Bogaard, M.J. Goumans, TGF-Beta and BMPR2 signaling in PAH: two black sheep in one family, Int. J. Mol. Sci. 19 (2018).

[12] F. Feng, R.L. Harper, P.N. Reynolds, BMPR2 gene delivery reduces mutation-related PAH and counteracts TGF-beta-mediated pulmonary cell signalling, Respirology 21 (2016) 526–532.

[13] J.Y. Sim, Nitric oxide and pulmonary hypertension, Korean J Anesthesiol 58 (2010) 4–14.

[14] K.M. Channon, H. Qian, S.E. George, Nitric oxide synthase in atherosclerosis and vascular injury: insights from experimental gene therapy, Arterioscler. Thromb. Vasc. Biol. 20 (2000) 1873–1881.

[15] P.M. Vanhoutte, Y. Zhao, A. Xu, S.W. Leung, Thirty years of saying NO: sources, fate, actions, and misfortunes of the endothelium-derived vasodilator mediator, Circ. Res. 119 (2016) 375–396.

[16] J.R. Klinger, S.H. Abman, M.T. Gladwin, Nitric oxide deficiency and endothelial dysfunction in pulmonary arterial hypertension, Am. J. Respir. Crit. Care Med. 188 (2013) 639–646.

[17] W. Xu, F.T. Kaneko, S. Zheng, S.A. Comhair, A.J. Janocha, T. Goggans, F. B. Thunnissen, C. Farver, S.L. Hazen, C. Jennings, R.A. Dweik, A.C. Arroliga, S. C. Erzurum, Increased arginase II and decreased NO synthesis in endothelial cells of patients with pulmonary arterial hypertension, Faseb. J. 18 (2004) 1746–1748.

[18] A. Tettey, Y. Jiang, X. Li, Y. Li, Therapy for pulmonary arterial hypertension: glance on nitric oxide pathway, Front. Pharmacol. 12 (2021), 767002.

[19] Q. Zhao, J. Zhang, H. Wang, PGC-1α overexpression suppresses blood pressure elevation in DOCA-salt hypertensive mice, Biosci. Rep. 35 (2015).

[20] J.X. Ye, S.S. Wang, M. Ge, D.J. Wang, Suppression of endothelial PGC-1α is associated with hypoxia-induced endothelial dysfunction and provides a new therapeutic target in pulmonary arterial hypertension, Am. J. Physiol. Lung Cell Mol. Physiol. 310 (2016) L1233–L1242.

[21] M. Mata, I. Sarrion, L. Milian, G. Juan, M. Ramon, D. Naufal, J. Gil, F. Ridocci, O. Fabregat-Andrés, J. Cortijo, PGC-1α induction in pulmonary arterial hypertension, Oxid. Med. Cell. Longev. 2012 (2012), 236572.

[22] N. Sawada, A. Jiang, F. Takizawa, A. Safdar, A. Manika, Y. Tesmenitsky, K.T. Kang, J. Bischoff, H. Kalwa, J.L. Sartoretto, Y. Kamei, L.E. Benjamin, H. Watada, Y. Ogawa, Y. Higashikuni, C.W. Kessinger, F.A. Jaffer, T. Michel, M. Sata, K. Croce, R. Tanaka, Z. Arany, Endothelial PGC-1α mediates vascular dysfunction in diabetes, Cell Metabol. 19 (2014) 246–258.

[23] S.M. Craige, S. Kröller-Schön, C. Li, S. Kant, S. Cai, K. Chen, M.M. Contractor, Y. Pei, E. Schulz, J.F. Keaney Jr., PGC-1α dictates endothelial function through regulation of eNOS expression, Sci. Rep. 6 (2016), 38210.

[24] J. Li, X.Y. Geng, X.L. Cong, PGC-1α ameliorates AngiotensinII-induced eNOS dysfunction in human aortic endothelial cells, Vasc. Pharmacol. 83 (2016) 90–97.

[25] S.H. Vitali, G. Hansmann, C. Rose, A. Fernandez-Gonzalez, A. Scheid, S.A. Mitsialis, S. Kourembanas, The Sugen 5416/hypoxia mouse model of pulmonary hypertension revisited: long-term follow-up, Pulm. Circ. 4 (2014) 619–629.

[26] N. Mouraret, E. Marcos, S. Abid, G. Gary-Bobo, M. Saker, A. Houssaini, J.L. Dubois-Rande, L. Boyer, J. Boczkowski, G. Derumeaux, V. Amsellem, S. Adnot, Activation of lung p53 by Nutlin-3a prevents and reverses experimental pulmonary hypertension, Circulation 127 (2013) 1664–1676.

[27] X. Zhang, H. Jin, X. Huang, B. Chaurasiya, D. Dong, T.P. Shanley, Y.Y. Zhao, Robust genome editing in adult vascular endothelium by nanoparticle delivery of CRISPR-Cas9 plasmid DNA, Cell Rep. 38 (2022), 110196.

[28] M.J. Bernas, F.L. Cardoso, S.K. Daley, M.E. Weinand, A.R. Campos, A.J. Ferreira, J. B. Hoying, M.H. Witte, D. Brites, Y. Persidsky, S.H. Ramirez, M.A. Brito, Establishment of primary cultures of human brain microvascular endothelial cells to provide an in vitro cellular model of the blood-brain barrier, Nat. Protoc. 5 (2010) 1265–1272.

[29] M.E. LeBlanc, W. Wang, X. Chen, Y. Ji, A. Shakya, C. Shen, C. Zhang, V. Gonzalez, M. Brewer, J.X. Ma, R. Wen, F. Zhang, W. Li, The regulatory role of hepatoma-derived growth factor as an angiogenic factor in the eye, Mol. Vis. 22 (2016) 374–386.

[30] H.B. Thibault, B. Kurtz, M.J. Raher, R.S. Shaik, A. Waxman, G. Derumeaux, E. F. Halpern, K.D. Bloch, M. Scherrer-Crosbie, Noninvasive assessment of murine pulmonary arterial pressure: validation and application to models of pulmonary hypertension, Circ Cardiovasc Imaging 3 (2010) 157–163.

[31] J.M. Gardin, F.M. Siri, R.N. Kitsis, J.G. Edwards, L.A. Leinwand, Echocardiographic assessment of left ventricular mass and systolic function in mice, Circ. Res. 76 (1995) 907–914.

[32] I. Strielkov, N.C. Krause, N. Sommer, R.T. Schermuly, H.A. Ghofrani, F. Grimminger, T. Gudermann, A. Dietrich, N. Weissmann, Hypoxic pulmonary vasoconstriction in isolated mouse pulmonary arterial vessels, Exp. Physiol. 103 (2018) 1185–1191.

[33] M. Shahid, E.S. Buys, Assessing murine resistance artery function using pressure myography, JoVE 76 (2013) 50328, https://doi.org/10.3791/50328.

[34] Y. Kawashima, Y. Kodera, A. Singh, M. Matsumoto, H. Matsumoto, Efficient extraction of proteins from formalin-fixed paraffin-embedded tissues requires higher concentration of tris(hydroxymethyl)aminomethane, Clin. Proteonomics 11 (2014) 4.

[35] C. Wolff, C. Schott, P. Porschewski, B. Reischauer, K.F. Becker, Successful protein extraction from over-fixed and long-term stored formalin-fixed tissues, PLoS One 6 (2011), e16353.

[36] V.H. Kumar, S. Lakshminrusimha, S. Kishkurno, B.S. Paturi, S.F. Gugino, L. Nielsen, H. Wang, R.M. Ryan, Neonatal hyperoxia increases airway reactivity and inflammation in adult mice, Pediatr. Pulmonol. 51 (2016) 1131–1141.

[37] R. Quarck, F. Perros, Rescuing BMPR2-driven endothelial dysfunction in PAH: a novel treatment strategy for the future? Stem Cell Invest. 4 (2017) 56.

[38] J.G. Cho, A. Lee, W. Chang, M.S. Lee, J. Kim, Endothelial to mesenchymal transition represents a key link in the interaction between inflammation and endothelial dysfunction, Front. Immunol. 9 (2018) 294.

[39] K. Nahar, J. Rashid, S. Absar, F.I. Al-Saikhan, F. Ahsan, Liposomal aerosols of nitric oxide (NO) donor as a long-acting substitute for the ultra-short-acting inhaled NO in the treatment of PAH, Pharm. Res. (N. Y.) 33 (2016) 1696–1710.
[40] E.D. Michelakis, Soluble guanylate cyclase stimulators as a potential therapy for PAH: enthusiasm, pragmatism and concern, Eur. Respir. J. 33 (2009) 717–721.
[41] Z. Li, S.A. Jimenez, Protein kinase Cdelta and c-Abl kinase are required for transforming growth factor beta induction of endothelial-mesenchymal transition in vitro, Arthritis Rheum. 63 (2011) 2473–2483.